Articles
doi.org/10.1002/batt.202000005

Chemistry Europe
European Chemical Societies Publishing

Special Collection

# Optimizing Calcium Electrolytes by Solvent Manipulation for Calcium Batteries

Kevin V. Nielson,[a] Jian Luo,[a] and T. Leo Liu*[a]

Calcium is a highly attractive metal anode because of its high earth abundance and low reduction potential. However, the lack of calcium electrolytes for reversible calcium deposition significantly hampers the development of Ca rechargeable batteries. Herein, the calcium deposition/stripping behaviors of a calcium salt electrolyte, $Ca[B(hfip)_4]_2$ ($[B(hfip)_4]^- =$ tetrakis (hexafluoroisopropyloxy)borate) were systematically studied using different working electrodes (GC, Pt, Cu, and Al) and different solvents including tetrahydrofuran (THF), dimethoxyethane (DME), and diglyme (DGM). It was found that the $Ca[B(hfip)_4]_2$/DGM electrolyte demonstrated the highest reversibility and stability in cyclic voltammetry and symmetric Ca/Ca half-cell studies. The $Ca[B(hfip)_4]_2$/DGM electrolyte was further employed to demonstrate a 3.4 V Ca battery using a $FePO_4$ cathode with a discharge capacity of 120 Ah/mg.

## 1. Introduction

Multivalent batteries have received increasing attention in order to developing post Li-ion battery technologies with high energy densities, low materials costs, and good cycling performance.[1–4] Particularly, significant advances have been made in developing electrolyte chemistry for Mg batteries.[1,3,5–19] However, high Lewis acidity of $Mg^{2+}$ ions makes them extremely challenging to adopt to the intercalation chemistry of Li ion batteries. Identifying suitable $Mg^{2+}$ ion intercalation cathode hosts with high kinetics and high redox potentials presents a formidable task.[2,4] Compared to $Mg^{2+}$, $Ca^{2+}$ with lower Lewis acidity is believed to be promising for intercalation chemistries.[20] In addition, Ca metal has a low reduction potential close to Li (+0.17 V vs Li) and also has the distinct advantages of divalent redox couple $Ca^{2+/0}$ giving it high gravimetric (ca. 1337 mAh/g) and volumetric capacities (2099 mAh/cm$^3$).[20] There are very limited efforts in developing Ca electrolytes for reversible Ca deposition, a prerequisite for developing Ca metal batteries.[20–25] $Ca(BF_4)_2$ in carbonate electrolytes was reported for Ca deposition and exhibited a degree of reversibility of less than 40% coulombic efficiency at 100 °C.[21] $Ca(BH_4)_2$ in THF was reported as the first example enabling reversible Ca deposition at room temperature albeit a low anodic stability of 2.4 V vs Ca due to the highly reducing nature of the $BH_4^-$ anion.[22,25] Recently Zhao-Karger and Nazar research groups simultaneously published their results describing a room temperature reversible Ca electrolyte $Ca[B(hfip)_4]_2$ (hfip = tetrakis(hexafluoroisopropyloxy)borate) in DME with an impressive anodic stability of above 4.0 V.[23,24] It is worth noting this unique $Ca[B(hfip)_4]_2$ electrolyte was inspired by prior studies of corresponding $Mg[Al(hfip)_4]_2$[8] and Mg $[B(hfip)_4]_2$[10] electrolytes.[20] Both research groups used DME solvent and a noble metal working electrode to demonstrate their reversible cyclic voltammetry curves. The authors did not however inspect the electrochemical deposition behaviors of the $Ca[B(hfip)_4]_2$ electrolyte using non-noble working electrode materials. In addition, the solvent effect of the $Ca[B(hfip)_4]_2$ electrolyte remains unexplored. Herein, we present a systematic study of the calcium deposition/stripping behaviors of the $Ca[B(hfip)_4]_2$ calcium salt electrolyte using different working electrodes (GC, Pt, Cu, and Al) and different solvents, tetrahydrofuran (THF), dimethoxyethane (DME) and diglyme (DGM). We found that DGM, a tridendate ligand solvent molecule, enables $Ca[B(hfip)_4]_2$ to manifest superior reversible and smooth Ca deposition even with a non-noble Cu working electrode.

## 2. Results and Discussion

The development of the $Ca[B(hfip)_4]_2$ electrolyte by Zhao-Karger and Nazar research groups were inspired by its Mg electrolyte congeners.[8,10] In fact, we also briefly studied this $Ca[B(hfip)_4]_2$ electrolyte using a glassy carbon electrode (Figure 1A) when we investigated Cl-free, non-corrosive Mg electrolytes supported by weakly coordinating anions.[6] However, the poor coulombic efficiency (33%) and large overpotential were (500 mV) observed and discouraged further pursuit. The studies of the $Ca[B(hfip)_4]_2$ electrolyte using Pt and Au electrodes by Zhao-Karger and Nazar research groups, respectively, yielded improved overpotential than our initial results with glassy carbon.[23,24] Thereby, we were promoted to study how working electrodes affect deposition electrochemistry of the $Ca[B(hfip)_4]_2$ electrolyte. At first, we established a baseline result by testing the $Ca[B(hfip)_4]_2$ electrolyte in DME using a Pt working electrode. A coulombic efficiency of 80% percent was calcu-

[a] K. V. Nielson, Dr. J. Luo, Prof. Dr. T. L. Liu
Department of Chemistry and Biochemistry
Utah State University,
Logan, Utah, 84318, USA
E-mail: leo.liu@usu.edu
liutbrss@gmail.com

Supporting information for this article is available on the WWW under https://doi.org/10.1002/batt.202000005

Special Collection An invited contribution to a Special Collection on Electrolytes for Electrochemical Energy Storage

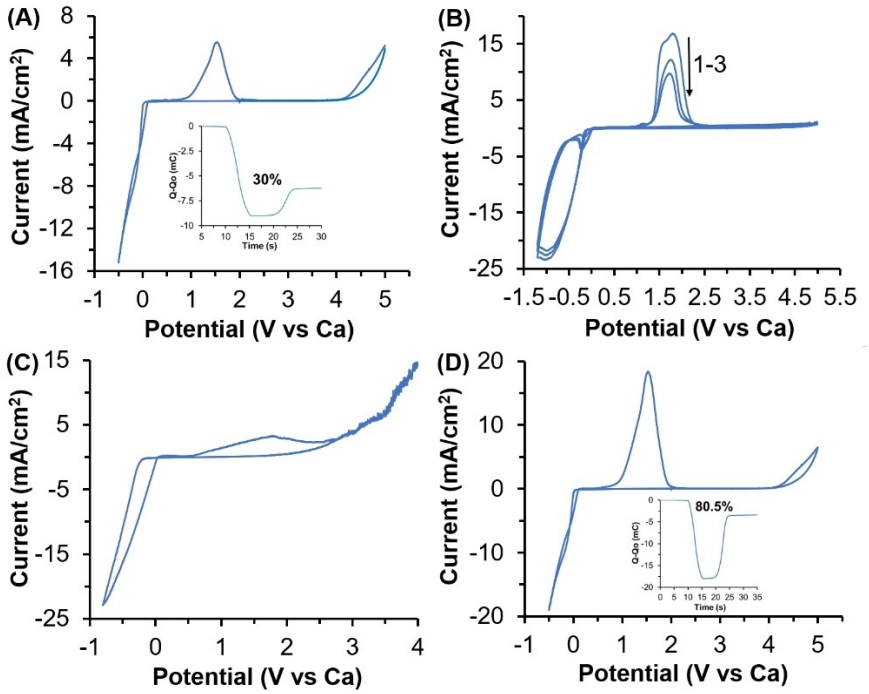


**Figure 1.** Cyclic voltammetry of a 0.25 M Ca[B(hfip)$_4$]$_2$/**DME** electrolyte solution with a glassy carbon rod counter electrode and a Ca reference electrode for A) Glassy carbon working electrode with Coulombic efficiency shown. B) Al working electrode with three cycles of decreasing current shown.C) Cu working electrode with limited reversibility and oxidation stability. D) Pt working electrode with inset showing accumulation of charge and Coulombic efficiency.

lated by summing up the total charge passed in the deposition and stripping processes (Figure 1D), and overpotential between the deposition and stripping was recorded as 0.33 V. These performance metrics are indeed better than the results collected by GC while Pt and GC displayed comparable anodic stability above 4.0 vs Ca. Since it is unreasonable that noble metals such as Pt or Au would be used in practical battery applications, we set out to test the reversibility of this electrolyte upon the surface of more common materials found in batteries. Al foil, a common current collector in Li-ion batteries, was tested as working electrode in the electrolyte. A very high overpotential ($>$1.0 V) was observed and current observed on stripping decreased dramatically over three cycles (Figure 1B) with a coulombic efficiency less than 40%. However, anodic current with the Al electrode was not observed even above 4.5 V vs Ca. Then another common current collector, Cu foil, was tested in the same conditions. The reversibility of deposition/stripping (25%) on the Cu electrode was negligible and continuous oxidative decomposition was observed beyond 2.5 V vs Ca (Figure 1C). In addition, we hypothesized that electrolyte decomposition at reducing potential is responsible for the low coulombic efficiencies. To test this theory, cyclic voltammetry was performed at increasingly reductive potentials using the Pt electrode. Accordingly, the coulombic efficiencies dropped to lower values as the cyclic voltammetry swept to lower voltages (Figure S1). This behavior may be deleterious to high voltage or fast charging battery applications where the battery anode can experience low reduction potential.

To further optimize the electrolyte stability, different ethereal solvents were tested to see if there was a solvent effect on electrolyte decomposition. 0.25 M Ca[B(hfip)$_4$]$_2$/THF was tested under the same conditions as the electrolyte in DME. A lower reversibility was observed up to 60% coulombic efficiency on a Pt electrode (Figure S2A). However, when the CV scan was directed to more negative voltages ($-$1.0 V vs Ca), the reversibility completely disappeared (Figure S2B). This result suggested that Ca[B(hfip)$_4$]$_2$ electrolyte had even worse reductive stability and reversibility in THF vs the DME electrolyte. It was proposed by Liao *et al.* that polydentate glyme can stabilize cations from interfering counter anions in Mg electrolytes.[19] Since THF is a lower coordinating solvent than DME and the stability was decreased, we then chose diglyme (DGM, a tridentate ligand solvent) to test the electrolyte. DGM is also advantageous with its higher boiling point and lower vapor pressure than THF and DME solvents. A 0.25 M Ca[B(hfip)$_4$]$_2$/DGM electrolyte was tested as the samples before.[8,10] To our delight, the electrolyte in DGM showed promising improvements over the tests in DME even on non-noble working electrode surfaces. A coulombic efficiency of 85.5% was calculated along with ca. 4.2 V anodic stability for the glassy carbon electrode (Figure 2A). On Cu foil, the Coulombic efficiency was 76% (Figure 2C) and on Al it was over 60% (Figure 2B) which are both much better than the negligible reversibility observed in DME solvent. The DGM electrolyte had over 80% Coulombic efficiency and an anodic stability of near 5.0 V on a Pt electrode surface comparable to the literature report in DME (Figure 2D).

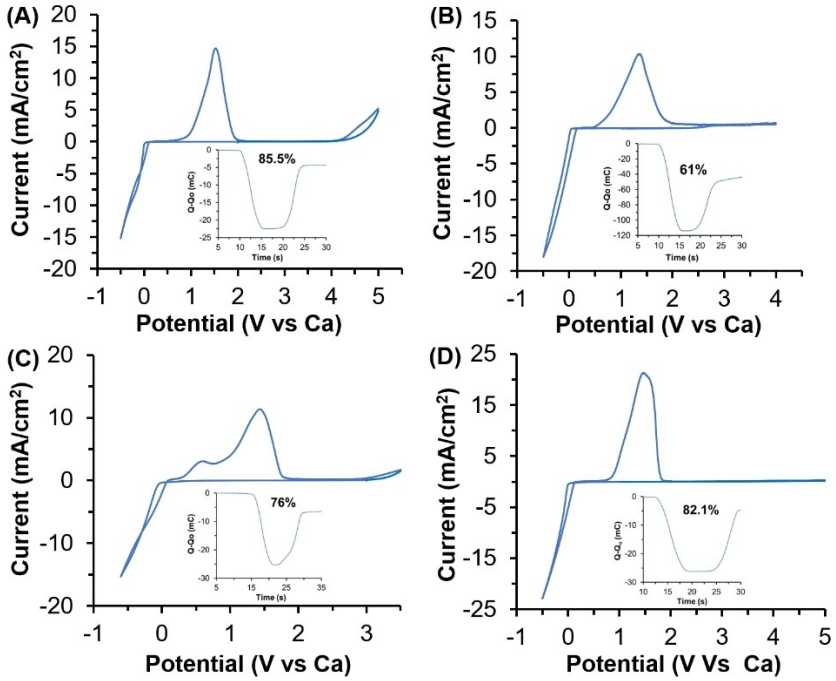


**Figure 2.** Cyclic voltammetry of a 0.25 M $Ca[B(hfip)_4]_2$/DGM electrolyte solution with glassy carbon rod counter electrode and a Ca reference electrode for A) Glassy Carbon working electrode. B) Al working electrode with inset showing accumulation of charge and Coulombic efficiency. C) Cu working electrode with Coulombic efficiency inset. D) Pt working electrode with Coulombic efficiency inset. All samples were cycled at 100 mV/s scan rate.

The electrolyte in the three different solvents was further tested in symmetric Ca/Ca cells using Ca deposited on Cu serving as both electrodes. The Current density was 1.0 mA/cm$^2$ for ten cycles then increased to 2.0, 4.0, and finally 8.0 mA/cm$^2$ while the overpotential of the cells was recorded. The cell with THF began to show voltage spikes greater than 1.0 V after 75 hours of cycling that became very severe ($>$3.0 V) at 8.0 mA/cm$^2$ and caused failing after 170 hours (Figure 3C). The DME containing cell showed similar behavior to the THF cell. Voltage spikes greater than 3.0 V were observed at 4.0 mA/cm$^2$ current density and $>$3.0 V spikes in overpotential were observed after 170 hours even at 1.0 mA/cm$^2$ current density. The DME containing cell failed after 220 hours (Figure 3B). The DGM electrolyte based cell had better performance than both THF and DME electrolyte based cells. The DGM electrolyte based cell (Figure 3A) never had voltage spikes greater than 0.5 V even at 8.0 mA/cm$^2$ and remained stable with less than 100 mV overpotential at 1.0 mA/cm$^2$ for the entire 300 hours of testing. The spikes are believed due to the increased cell resistance and resulting polarization at high current. According to the SEM and EDX studies (see Figure 4 below), it is believed that the electrolyte decomposition was accelerated at high current in the cells using the $Ca[B(hfip)_4]_2$/DME and $Ca[B(hfip)_4]_2$/THF electrolytes and led the formation of insulate $CaF_2$ (and possible organic) deposits on the electrode surface.

Scanning electron microscopy (SEM) was employed to probe the mode of failure for the symmetric cells containing THF and DME solvents (Figure 4). Calcium dendrites observed on the current collector interface were observed for the DME electrolyte cell (Figure 4B) while the current collectors from the THF cell did not show dendrite formation (Figure 4A). Thus we propose the cell failure in THF and DME was caused by passivation from decomposed electrolyte. Actually, the deposition on Cu with THF solvent was very smooth and uniform. Only upon inspection of the elemental mapping it was observed that the atomic ratio of fluorine was much higher compared to Ca than the other samples suggesting that the majority of deposition in THF solvent is actually $CaF_2$ rather than Ca metal. This observation is consistent with the complete lack of an oxygen signal from the THF sample where the Ca metal oxidized quickly in the atmosphere for the DGM and DME samples. In contrast, the $CaF_2$ did not undergo the same oxygenation process. The DGM cell also did not have dendritic growths but rather had islands of Ca and $CaF_2$ deposited in particle like morphologies (Figure 4C).

After the assessments of reversibility and stability of $Ca[B(hfip)_4]_2$ electrolyte in three different solvents, it became of great interest to test the electrolyte in a full cell Ca metal battery configuration. An $FePO_4$ cathode was prepared by electrochemical delithiation of $LiFePO_4$ then was used as a Ca host. Ca metal deposited on Cu foil was used as the anode, a glass fiber separator was used as separator, and 0.25 M $Ca[B(hfip)_4]_2$/DGM was used as the electrolyte in a coin cell. The cell had a very high initial charge capacity possibly due to SEI formation. Then the cell was continuously tested for 10 cycles with up to a discharge capacity of 120 mAh/g and a coulombic efficiency of up to 70% (Figure 5A). The representative charge/discharge curves are given in Figure 5B, and indicates a cell voltage of 3.4 V for the $Ca/FePO_4/Ca[B(hfip)_4]_2$ battery. The cycling performance of the cell remains to be further improved

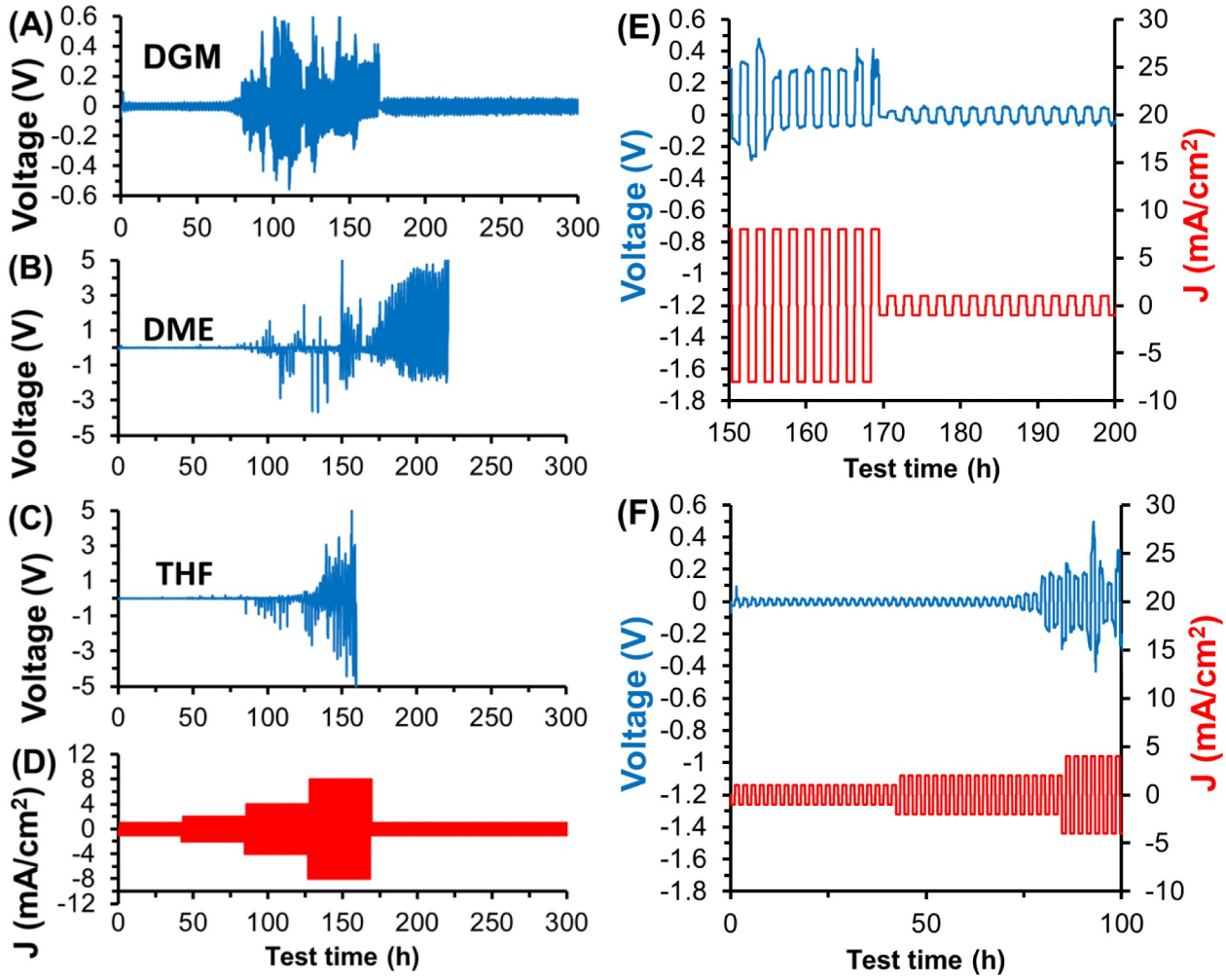


**Figure 3.** Symmetric cell evaluation of $Ca[B(hfip)_4]_2$ in different solvents with Ca deposited on Cu serving as both electrodes for A) DGM, B) DME, C) THF. D) Test time and current density for the three cells, E) end cycling for DGM cell, and F) initial cycling of DGM cell.

but it wasdemonstrated that $Ca[B(hfip)_4]_2$/DGM could be used in a high voltage (4.0 V) application (Figure 5C) with sufficient anodic reversibility to achieve a relativity high discharge capacity for $FePO_4$ cathode (Figure 5B). EDX mapping confirmed the $Ca^{2+}$ presence in the $FePO_4$ cathode and was also used to calculate the amount of $Ca^{2+}$ insertion in the $FePO_4$ cathode (Figure S3). The calculated ratio was Ca:Fe 0.43:1, giving a formula of $Ca_{0.43}FePO_4$ for the discharged state. ICP-MS was further employed to confirm the inserted Ca ions (0.43 equivalent for Fe) to the Fe Content and also suggests a small amount of $Li^+$ in the cathode material (Li:Ca $<$ 1:4). Table S1 provides the detailed element analysis of the calcinated $FePO_4$ cathode by EDX and ICP-MS. These preliminary Ca battery results give hope to improve long-term stability and coulombic efficiency through future optimization.

## 3. Conclusions

The $Ca[B(hfip)_4]_2$ electrolyte was tested using different electrodes in three different ethereal solvents to gage the current collector and solvent effects on the electrolyte stability. It was found that, the reversibility of Ca deposition and stripping of the $Ca[B(hfip)_4]_2$ electrolyte in DGM (compared to DME and THF) was greatly improved on common battery current collectors including Cu and Al and also on glassy carbon. Symmetric Ca|Ca cell studies also confirmed that the DGM solvent based electrolyte showed the lowest polarization at all current densities and had the longest cycling stability over 300 hours. Only the $Ca[B(hfip)_4]_2$/DGM cell had a smooth dendrite free morphology of mostly Ca deposits. These results suggest DGM may be a more suitable solvent for Ca electrolytes in future studies. In addition, a 3.4 V rechargeable Ca battery was demonstrated using the $Ca[B(hfip)_4]_2$/DGM electrolyte and an $FePO_4$ cathode. Our results highlight the important solvent effect in developing advanced Ca electrolytes to realize durable and energy dense Ca batteries.

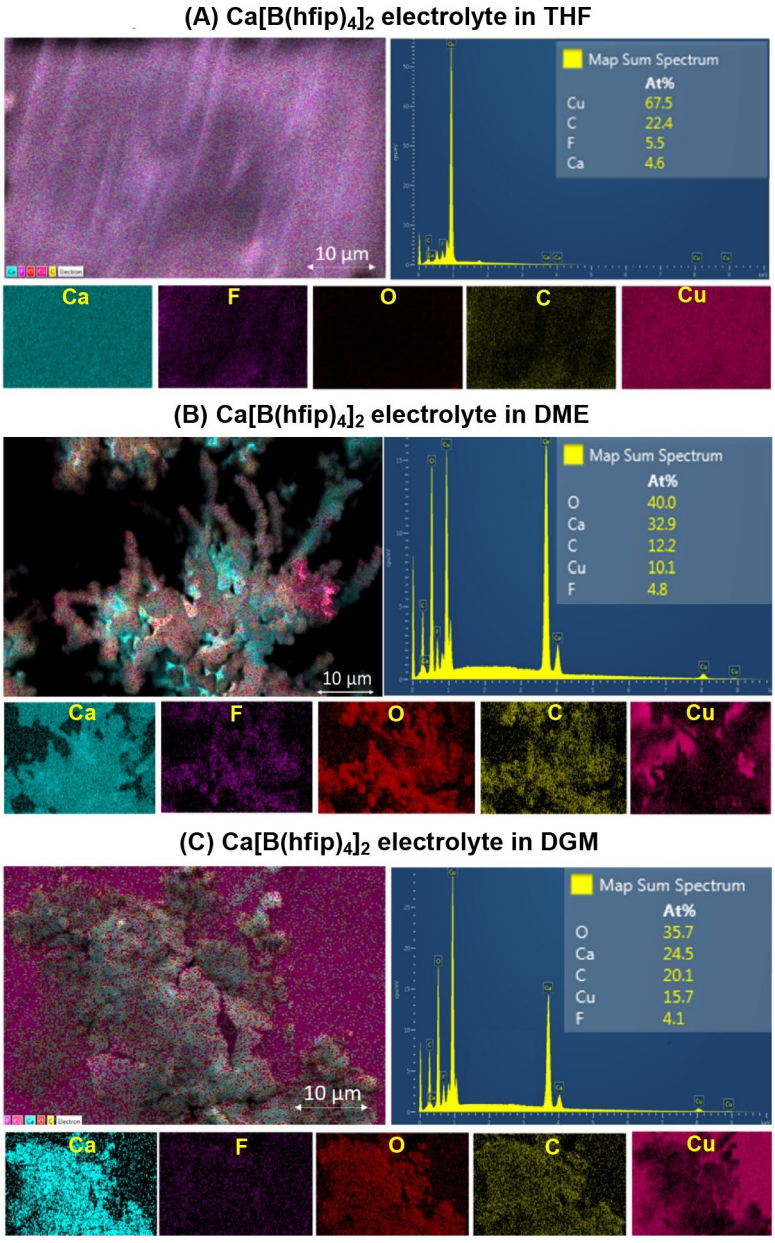


**Figure 4.** Post analysis by SEM and EDX elemental mapping of Cu current collectors from Ca | Ca symmetric cells for A) the cell using THF comprising mostly $CaF_2$ deposits, B) the cell using DME solvent with dendrites measured by a scale bar, and C) the cell using DGM solvent with smooth particle deposition morphology.

## Experimental Section

### Materials and operations

Chemicals and manipulations: $Ca(BH_4)_2 \cdot 2THF$ was purchased from TCI, dried at 100 °C in an Argon glovebox, and used directly. All experimental operations were conducted under an Argon atmosphere with $H_2O$ and $O_2$ concentrations below 0.1 ppm. Hexafluoroisopropanol was stored over activated molecular sieves (4 angstroms) for at least one week before use. All solvents were purified and dried by distillation over Na whereby the initial and final 10% of solvent was separated away for less solvent sensitive chemistry.

### Synthesis of $Ca[B(hfip)_4]_2 \cdot 4DME$

$Ca(BH_4)_2 \cdot 2THF$ (1.0 mmol, 214 mg) was added slowly over one hour to a 5.0 ml, ultra-dry DME solution containing hexafluoroisopropanol (8.0 mmol, 1.34 g). The reaction temperature was then increased to reflux for 4 hours. Solvent was removed under reduced pressure until visibly dry then further removed under vacuum at 80 °C for 6 hours. A fine white powder was obtained (1.13 g, 85.0%). $^{19}F$ NMR (500 MHz $CD_3CN$): $\delta = -75.4$. $^{11}B$ NMR ( 500 MHz, $CD_3CN$): $\delta = 8.78$(s).

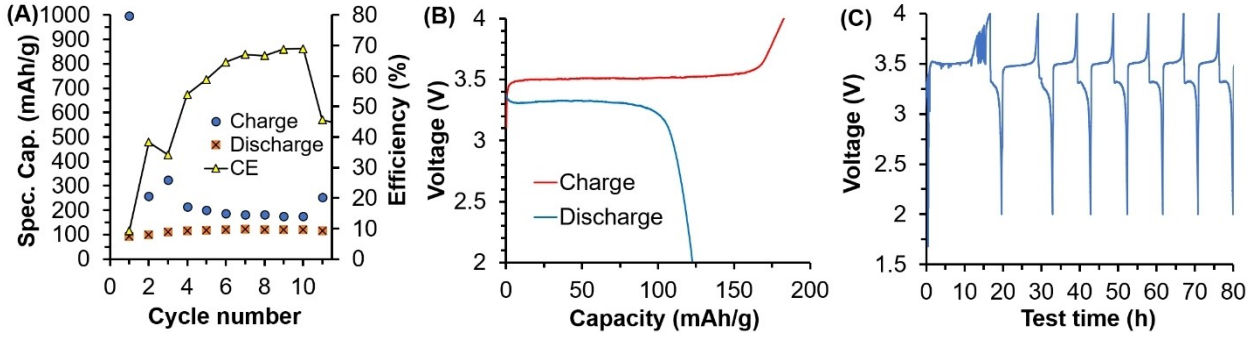


**Figure 5.** Electrochemical performance of a Ca/$FePO_4$ rechargeable battery with a 0.25 M $Ca[B(hfip)_4]_2$/DGM electrolyte at 10 mA/g for charging and discharging processes. A) Charging and discharging capacities and Coulombic efficiency. B) Representative charging/discharging curves of the seventh cycle. C) Charging/discharging voltage profile over testing time.

### Cyclic voltammetry tests

All electrochemical measurements were collected with a Gamry 1000E potentiostat. All cyclic voltammetry was conducted with a glassy carbon rod counter electrode and a Ca rod reference electrode. Working electrodes were one of the following: Pt disc, Al wire, Cu wire, or glassy carbon disk. All working electrodes were available commercially and used directly. All electrolytes were composed of 0.25 M $Ca(B(hfip)_4)_2$ in DME, THF, or DGM. All CV tests were conducted at 100 mV/s scan rate.

### SEM-EDS

SEM was done on a FEI Quanta FEG 650. SEM samples were prepared by scavenging current collectors from coin cells and affixing them to Carbon coated Al SEM sample substrates. Symmetric cells were assembled from Ca coated Cu foil as electrodes, glass fiber separator, and 50 uL specified electrolyte. All samples were soaked twice for 20 minutes in neat solvent according to which solvent (THF, DME, or DGM) was used for the electrolyte. The samples were loaded into a microscopy chamber under a cool stream of nitrogen that was quickly evacuated to less than $5*10^{-5}$ Torr pressure before the electron beam was initiated.

### Symmetric cell tests

Symmetric cells were assembled using CR2025 coin cells with glass fiber type A separators. Cu discs deposited with Ca was used as both electrodes. 0.25 M $Ca(B(hfip)_4)_2$ in either THF, DME, or DGM was used as the electrolyte. 50 uL electrolyte was used in all cells. Cells were tested galvanostatically at different current densities. A constant current was applied for one hour then the cell was rested for 10 minutes. Then the polarity was reversed and current was applied for one hour followed by 10 minutes resting time. A safety measure was programmed into the battery tester to discontinue testing if cell voltage exceeded plus or minus 5 volts. For DME and THF containing cells the battery testing was automatically halted when overpotentials exceeded 5.0 V. For DGM containing cells the polarization of the cell never exceeded 0.5 V and continued running for in excess of 300 hours.

### Battery tests

All batteries were tested on a Lanhe battery tester. Delithiated $FePO_4$ electrodes were prepared by electrochemical delithiation. 12 mm Aluminum discs containing $LiFePO_4$, carbon black acetylene, and PVDF binder in a weight ratio of 80:10:10 respectively were loaded into CR2025 type coin cells with Li metal anode and 1.0 M LiTFSI in 1:1 DME:DOL electrolyte (20 uL) with a glass fiber type A separator. The batteries were charged to 4.0 V with constant current of 1.0 mA/g. The cell was then dissembled and the cathode disc was soaked in neat DME for 20 minutes two times and then dried under vacuum at room temperature for one hour. The electrodes were then loaded into a new coin cell with Ca metal anode and 0.25 $Ca(B(hfip)_4)_2$ in THF, DME, or DGM electrolyte. Only the DGM containing cell could cycle as other solvent containing electrolytes did not allow the cell to charge with continuous current below 4.0 V vs Ca. The Ca metal batteries were cycled at 10 mA/g with respect to the cathode active material corresponding to a C rate of C/15.

## Acknowledgements

*We thank the financial support for this research by Utah State University faculty startup funds (to T.L.L.). We acknowledge that the NMR studies are supported by NSF MRI program (award number 1429195).*

## Conflict of Interest

The authors declare no conflict of interest.

**Keywords:** calcium batteries · calcium electrolytes · energy storage · solvation · weakly coordination anions

[1] S. He, K. V. Nielson, J. Luo, T. L. Liu, *Energy Storage Mater.* **2017**, *8*, 184–188.
[2] P. Canepa, G. Sai Gautam, D. C. Hannah, R. Malik, M. Liu, K. G. Gallagher, K. A. Persson, G. Ceder, *Chem. Rev.* **2017**, *117*, 4287–4341.
[3] K. Xu, *Chem. Rev.* **2014**, *114*, 11503–11618.
[4] M. Mao, T. Gao, S. Hou, C. Wang, *Chem. Soc. Rev.* **2018**, *47*, 8804–8841.
[5] J. Luo, S. He, T. L. Liu, *ACS Energy Lett.* **2017**, *2*, 1197–1202.
[6] J. Luo, Y. Bi, L. Zhang, X. Zhang, T. L. Liu, *Angew. Chem. Int. Ed.* **2019**, *58*, 6967–6971.
[7] T. Liu, Y. Shao, G. Li, M. Gu, J. Hu, S. Xu, Z. Nie, X. Chen, C. Wang, J. Liu, *J. Mater. Chem. A* **2014**, *2*, 3430–3438.
[8] J. T. Herb, C. A. Nist-Lund, C. B. Arnold, *ACS Energy Lett.* **2016**, *1*, 1227–1232.

[9] Z. Zhao-Karger, X. Zhao, D. Wang, T. Diemant, R. J. Behm, M. Fichtner, *Adv. Energy Mater.* **2015**, *5*, 1401155–1401163.
[10] Z. Zhao-Karger, M. E. Gil Bardaji, O. Fuhr, M. Fichtner, *J. Mater. Chem. A* **2017**, *5*, 10815–10820.
[11] K. A. See, K. W. Chapman, L. Zhu, K. M. Wiaderek, O. J. Borkiewicz, C. J. Barile, P. J. Chupas, A. A. Gewirth, *J. Am. Chem. Soc.* **2016**, *138*, 328–337.
[12] J. Wen, W. Shi, F. Zhang, D. Liu, S. Tang, H. Wang, X.-M. Lin, A. Lei, *Org. Lett.* **2017**, *19*, 3131–3134.
[13] L. C. Merrill, J. L. Schaefer, *Langmuir* **2017**, *33*, 9426–9433.
[14] L. C. Merrill, J. L. Schaefer, *Chem. Mater.* **2018**, *30*, 3971–3974.
[15] S. G. McArthur, L. Geng, J. Guo, V. Lavallo, *Inorg. Chem. Front.* **2015**, *2*, 1101–1104.
[16] R. Jay, A. W. Tomich, J. Zhang, Y. Zhao, A. De Gorostiza, V. Lavallo, J. Guo, *ACS Appl. Mater. Interfaces* **2019**, *11*, 11414–11420.
[17] O. Tutusaus, R. Mohtadi, T. S. Arthur, F. Mizuno, E. G. Nelson, Y. V. Sevryugina, *Angew. Chem. Int. Ed.* **2015**, *54*, 7900–7904.
[18] R. Davidson, A. Verma, D. Santos, F. Hao, C. Fincher, S. Xiang, J. Van Buskirk, K. Xie, M. Pharr, P. P. Mukherjee, S. Banerjee, *ACS Energy Lett.* **2019**, *4*, 375–376.
[19] K.-C. Lau, T. J. Seguin, E. V. Carino, N. T. Hahn, J. G. Connell, B. J. Ingram, K. A. Persson, K. R. Zavadil, C. Liao, *J. Electrochem. Soc.* **2019**, *166*, A1510-A1519.
[20] K. V. Nielson, J. Luo, T. L. Liu, *Angew. Chem. Int. Ed.* **2020**, *59*, DOI: 10.1002/anie.201913465.
[21] A. Ponrouch, C. Frontera, F. Bardé, M. R. Palacín, *Nat. Mater.* **2015**, *15*, 169.
[22] D. Wang, X. Gao, Y. Chen, L. Jin, C. Kuss, P. G. Bruce, *Nat. Mater.* **2017**, *17*, 16.
[23] Z. Li, O. Fuhr, M. Fichtner, Z. Zhao-Karger, *Energy Environ. Sci.* **2019**.
[24] A. Shyamsunder, L. E. Blanc, A. Assoud, L. F. Nazar, *ACS Energy Lett.* **2019**, *4*, 2271–2276.
[25] K. Ta, R. Zhang, M. Shin, R. T. Rooney, E. K. Neumann, A. A. Gewirth, *ACS Appl. Mater. Interfaces* **2019**, *11*, 21536–21542.

Manuscript received: January 7, 2020
Revised manuscript received: March 2, 2020
Accepted manuscript online: March 22, 2020
Version of record online: April 15, 2020